JOURNAL OF AIRCRAFT
Vol. 43, No. 4, July–August 2006

Robust Drag Minimization of Aerodynamic Wings in Engineering Environment

Sergey Peigin*
Israel Aircraft Industries, 70100 Ben-Gurion Airport, Israel
and
Boris Epstein†
Academic College of Tel-Aviv-Yaffo, 64044 Tel-Aviv, Israel

The multipoint aerodynamic design of transport-type wings is studied. The optimization was performed by means of the code OPTIMAS, which was recently developed by the authors in the industrial environment of Israel Aircraft Industries. The optimization method is based on the use of genetic algorithms, accurate full Navier–Stokes drag prediction, and efficient handling of practical aerodynamic and geometrical constraints. The results include a variety of optimization cases for aerodynamic design of transport-type wings.

I. Introduction

THE contribution of computational fluid dynamics (CFD) to aerodynamic design steadily grows due to continuing improvement in the accuracy and robustness of CFD simulations. The past three decades saw a radical change in the entire process of aerodynamic design due to the increasing role of CFD.

Until recently, the role of CFD in aerodynamic design was confined to flow analysis in a limited range of flight conditions and aerodynamic shapes. Additional limitations were caused by the variable accuracy level in the prediction of different aerodynamic characteristics. For example, accurate CFD estimation of drag and pitching moments of three-dimensional shapes became available only in recent years, during which the Navier–Stokes methods reached maturity, whereas reasonably accurate estimates of $\partial C_L/\partial\alpha$ were already accessible in the mid-1970s through linear panel methods.

The first attempts to introduce optimization tools to aerodynamic design were made as early as 1945. (See the classical work by Lighthill.[1]) More complicated CFD-driven optimization methods appeared over subsequent years.[2–7] Nevertheless, before the last few years, these methods had a very limited impact on three-dimensional design practice.

The reasons why the optimization tools are still not being exploited in the design process as one would like include the following: First, only recently has computational simulation been allowed for the relatively accurate drag prediction required in engineering practice. Second, the industrial optimization of aerodynamic shapes necessitates high-dimensional search spaces, and a large number of nonlinear constraints are placed on a desired optimum, which significantly increases the complexity of the problem. Additionally, the huge computational volume needed for practical optimization presents a serious obstacle to the incorporation of CFD-based optimization into the core of the industrial aerodynamic design.

The aircraft design process is generally divided into three stages: conceptual design, preliminary design, and final detailed design. The aerodynamic design plays a leading role during the preliminary design stage where the external aerodynamic shape is typically finalized. The final design would normally be carried out only on the commercially promising completion of the preliminary stage, which makes the preliminary design stage crucial for the overall success of the project.

The aerodynamic design process is embedded in the overall preliminary design with the starting point coming from the conceptual design. The inner loop of aerodynamic analysis is included within an outer (multidisciplinary) loop that is a part of a major design cycle. Because of the limitations of the overall design technology, this cycle is usually repeated a number of times.

Thus, the introduction of a CFD-driven robust automatic aerodynamic optimization that would allow for the reduction of the amount of design cycles would significantly shorten the overall design process.

One of major objectives of the preliminary design is to develop the minimum drag aircraft configuration at cruise conditions subject to various constraints implied by the conceptual design stage. This means that the use of an automatic optimizer that accurately satisfies various geometrical and aerodynamic constraints may not only reduce the design costs but also essentially improve the quality of design, thus considerably increaseing the probability that the following final design will result in a real aircraft.

That is why, in the last decade, optimal CFD-driven aerodynamic shape design has aroused steadily increasing interest in the research establishment.[8–11] From the industrial point of view, the most advanced results have been achieved by The Boeing Company,[12] where multipoint design has been used extensively for airplane development using full-potential/boundary-layer-based optimization.

The main objective of this paper is to present a new, efficient optimization tool for aerodynamic design that was successfully incorporated into the core of the preliminary design stage, based on full Navier–Stokes computations.

The power of the method is illustrated by the design of a number of two- and three-dimensional aerodynamic wings typical of a transport-type aircraft in a wide range of wing planforms and flight conditions. It is demonstrated that the proposed method allows for the design of practically feasible aerodynamic shapes that 1) possess a low drag at cruise conditions, 2) satisfy a significant number of geometrical and aerodynamic constraints (15–20 per design), and 3) offer a good off-design performance in markedly different flight conditions such as takeoff and high Mach zone.

This paper is organized as follows. In Sec. II, the problem formulation is given. In Sec. III the Israel Aircraft Industries (IAI) inhouse optimization method is briefly described. Numerical results are presented and analyzed in Sec. IV.

II. Statement of Problem

The starting point of the aerodynamic wing design cycle is an initial CAD geometry definition. In the first design cycle, this definition

Presented as Paper 2005-5082 at the Applied Aerodynamics Conference, Toronto, Canada, 6–9 June 2005; received 7 July 2005; revision received 11 October 2005; accepted for publication 12 October 2005.

*Professor, Engineering Division. Member AIAA.
†Professor, Computer Sciences Department. Member AIAA.

results from the conceptual design stage, which also provides the aerodynamic performance data. These include the prescribed cruise lift, Mach, altitude, and minimum allowed drag values that should ensure the aerodynamic goals of the aircraft mission (such as range, payload, fuel volume, etc.). The desired geometry is sought in the class of solutions that satisfy various geometrical, aerodynamic, and multidisciplinary constraints that also originate from the stage of conceptual design. Specifically, the constraints are usually placed on airfoils' thickness, maximum allowed pitching moment, minimum $C_L^{\max}$ at takeoff conditions, etc.

The objective of this cycle is to develop a wing geometry with as low a drag at cruise conditions as possible that, at the same time, satisfies the foregoing constraints.

The main idea behind the proposed approach is to accomplish this objective through a CFD-based solution of the properly formulated multipoint constrained optimization problem.

To state the present optimization problem correctly, it is important to clarify the nature of different constraints, their structure, and their interaction in the framework of this structure.

The set of constraints may be divided into the following two classes: the class of geometrical constraints and the class of aerodynamic constraints. The geometrical constraints are mostly independent of flight conditions and are easily verified, that is, the verification of the tested geometry is computationally cheap, whereas aerodynamic constraints naturally depend on flight conditions and necessitate heavy CFD runs for their verification. The aerodynamic constraints are subclassified into the constraints at the main design point (typically cruise conditions) and the constraints at off-design conditions.

The second important issue is the choice of the objective function. We assume that the drag coefficient C_D of a tested configuration is a sensitive and reliable indicator of its aerodynamic performance and, thus, we employ C_D as the objective function of the considered optimization problem.

The next basic principle is related to the implementation of constraints in the optimization algorithm. Where possible, the constraints should be satisfied exactly in a direct way, whereas the remaining constraints should be converted into alternative constraints that can be expressed in terms of drag. For example, we managed to satisfy the geometrical constraints and such aerodynamic constraints as the prescribed lift coefficient exactly, whereas the requirement of a sufficiently high $C_L^{\max}$ at takeoff conditions is reformulated in terms of drag at the corresponding flight conditions.

Finally, to ensure the accuracy of optimization, we require that, for any geometry feasible from the viewpoint of constraints, the value of the objective (cost) function remains exactly equal to the value of the drag coefficient without any penalization.

Based on the preceding principles, the mathematical formulation of the optimization problem whose solution allows achievement of the goal of the preliminary design cycle may be expressed as follows.

The objective of the general multipoint optimization problem is to minimize the weighted combination C_D^{wtd} of drag coeficients at the main design and secondary design points (flight conditions)

$$C_D^{\text{wtd}} = \sum_{k=1}^{K} w_k C_D(k)$$

where K is the total number of design points.

The solution is sought in the class of wing shapes subject to the following classes of constraints:

1) The first class of constraints is aerodynamic, such as prescribed constant total lift coefficient $C_L^*(k)$ and minimum allowed pitching moment $C_M^*(k)$,

$$C_L(k) = C_L^*(k), \qquad C_M(k) \geq C_M^*(k) \tag{1}$$

2) The second class of constraints is geometrical, impacting the shape of the wing surface in terms of properties of sectional airfoils at the prescribed wingspan locations: relative thickness $(t/c)_i$, relative local thickness $(\Delta y/c)_{ij}$ at the given chord locations $(x/c)_{ij}$ (beams constraints), relative radius of leading edge $(R/c)_i$, and trailing-edge angle θ_i,

$$(t/c)_i \geq (t/c)_i^*, \qquad (\Delta y/c)_{ij} \geq (\Delta y/c)_{ij}^*, \qquad (R/c)_i \geq (R/c)_i^*$$

$$\theta_i \geq \theta_i^*, \qquad i = 1, \ldots, N_{ws}, \qquad j = 1, \ldots, N_{\text{BC}}(i) \tag{2}$$

where N_{ws} is the total number of sectional airfoils subject to optimization, $N_{\text{BC}}(i)$ is the total number of beams constraints at section i, and values $(t/c)_i^*, (\Delta y/c)_{ij}^*, \theta_i^*, (R/c)_i^*, C_L^*$, and C_M^* are prescribed parameters of the problem.

Thus, in the present work the total number of considered constraints N_{cs} is equal to

$$N_{cs} = 2 \times K + 3 \times N_{ws} + \sum_{i=1}^{N_{ws}} N_{\text{BC}}(i)$$

In principle, the present optimization method allows for handling a large number of constraints of different natures in addition to the aforementioned ones.

As a gasdynamic model for calculating C_D, C_L, and C_M values, the full Navier–Stokes equations are used. Numerical solution of the full Navier–Stokes equations was based on a multiblock code NES[13] that employs structured point-to-point matched grids. The code is based on the essentially nonoscillatory concept with a flux interpolation technique[14] that allows for accurate estimation of sensitive aerodynamic characteristics such as lift, pressure drag, friction drag, and pitching moment.

The code ensures high accuracy of the Navier–Stokes computations and high robustness for a wide range of flows and geometrical configurations. The high performance of NES was systematically demonstrated by testing it in a wide range of aerodynamic configurations of different complexity: from one-element two-dimensional airfoils (such as NACA0012 and RAE2822) through the ONERA M6 wing, transport-type supercritical wings, and ARA M100 wing-body geometry[13] to complex wing–body–nacelle–pylon DLR-F6 aircraft configurations.[15]

III. Optimization Method

In this section, we briefly describe the optimization method developed by the authors at IAI. The method forms the basis for the optimization tool OPTIMAS. A detailed description of the method may be found in Refs. 16 and 17.

The optimization technique employed genetic algorithms (GAs) in combination with a reduced-order models (ROM) method based on local databases obtained by full Navier–Stokes computations. The main features of the present multipoint optimization method include a new strategy for efficient handling of nonlinear constraints in the framework of GAs, scanning of the optimization search space by a combination of full Navier–Stokes computations with the ROM method, and multilevel parallelization of the whole computational framework, which efficiently makes use of computational power supplied by massively parallel processors.

As a basic algorithm, a variant of the floating-point GA (Ref. 18) is used. The mating pool is formed through the use of tournament selection. We employ the arithmetical crossover, the nonuniform real-coded mutation defined by Michalewicz,[18] a distance-dependent mutation operator,[19] and the elitism principle.

In the considered optimization problem, the presence of constraints has a great impact on the solution. This is because the optimal solution does not represent a local minimum in the conventional sense of the word. Instead, it is located on an intersection of hypersurfaces of different dimensions, generated by linear and non-linear constraints. Additionally, the problem of finding such an extremum is essentially complicated by the fact that these hypersurfaces, which bound the feasible search space, are not known in advance and may possess irregular topology.

For example, it is quite clear that in the problem defined in Sec. II, with no constraints imposed on the wing thickness, the optimal wing should be infinitely thin. Thus, it is aerodynamically expected that in the case of the thickness-constrained optimization, the optimal

wing will possess the minimum allowed thickness. This implies that the optimal point should reside exactly on the corresponding hypersurface.

In the case of constraints, imposed on the aerodynamic characteristics such as pitching moment C_M, the situation is even less controlled. Similar to the preceding example, the optimal solution should be found exactly on the constraint boundary. However, contrary to the case of geometrical constraints, the determination of the boundary is a much heavier computational problem. For geometrical constraints, the feasibility test is computationally very cheap, whereas in the case of aerodynamic constraints, the corresponding test requires a full (computationally heavy) CFD run.

Unfortunately, in their basic form, GAs are not capable of handling constraint functions limiting the set of feasible solutions. To resolve this, a new approach is suggested that can be basically outlined as follows. (For further details see Ref. 20.)

1) Change the conventional search strategy by employing search paths that pass through both feasible and infeasible points (instead of the traditional approach where only feasible points may be included in a path).

2) To implement the new strategy, it is proposed to extend the search space. This requires the evaluation (in terms of fitness) of the points that do not satisfy the constraints imposed by the optimization problem. A needed extension of an objective function may be implemented by means of GAs due to their basic property: Contrary to classical optimization methods, GAs are not confined to only smooth extensions.

One of the main weaknesses of GAs lies in their poor computational efficiency. This prevents their practical use in cases where the evaluation of the cost function is computationally expensive as happens in the framework of the full Navier–Stokes model, even in the two-dimensional case.

To overcome this, we introduce an intermediate computational agent: a computational tool that, on the one hand, is based on a very limited number of exact evaluations of an objective function and, on the other hand, provides a fast and reasonably accurate computational feedback in the framework of a GA search.

In this work, we use ROM approach in the form of local approximation method (LAM). With the ROM-LAM, the solution functionals that determine a cost function and aerodynamic constraints (such as pitching moment, lift, and drag coefficients), are approximated by a local database. The database is obtained by solving the full Navier–Stokes equations in a discrete neighborhood of a basic point positioned in the search space.

To ensure the accuracy and robustness of the method, a multidomain prediction–verification principle is employed. That is, on the prediction stage, the genetic optimum search is concurrently performed on a number of search domains. As the result, each domain produces an optimal point, and the whole set of these points is verified (through full Navier–Stokes computations) in the verification stage of the method. Thus, the final optimal point is determined.

To ensure the global character of the search, it is necessary to overcome the local nature of the preceding approximation. For this purpose, it is suggested that iterations be performed in such a way that in each iteration, the result of optimization serves as the initial point for the next iteration step (further referred to as an optimization step).

One of key difficulties in the implementation of optimization algorithms arises because, roughly speaking, each CFD run requires a different geometry and, therefore, the construction of a new computational grid. For novel complex geometries, meshes are generally constructed manually, which is very time consuming.

To overcome this obstacle and maintain the continuity of the optimization stream, we made use of the topological similarity of geometrical configurations (involved in the optimization process) such that the grids are constructed by means of a fast automatic transformation of the initial grid that corresponds to the starting basic geometry.

The problem of optimization of aerodynamic shapes is very time consuming because it requires a huge amount of computational work. Each optimization step requires a number of heavy CFD runs, and a large number of such steps is needed to reach an optimum. Thus, the construction of a computationally efficient algorithm is vital for the success of the method in an engineering environment.

To achieve this goal, a multilevel parallelization strategy[21] was used. It includes parallelization of the multiblock full Navier–Stokes solver (see Ref. 22), parallel evaluation of objective function, and, finally, parallelization of the optimization framework.

From the industrial viewpoint, the optimization method by itself (described in the preceding section) only forms a basis for the design cycle optimization process. To be successfully incorporated into practical aerodynamic design, it must be complemented by additional tools, which should ensure the continuity and the technical feasibility of the overall procedure in terms of accuracy, robustness, cost, and time schedule. Thus, we deal with a technology that should ensure the achievement of the preliminary design cycle goals.

Over the course of the entire technology cycle, from the very beginning to final production, the geometry of the aerodynamic shape is the main object of continuous modification. With this end in view, the preceding requirements to the preliminary design technology must be reformulated in terms of shape modification.

Specifically, the technology process may be divided into a number of successive stages. In each stage, the ouput geometry of the preceding stage constitutes an input geometry to the next stage.

For example, the final geometry coming from the conceptual design cycle is an initial geometry to the stage responsible for the construction of computational grids. In this stage, the input format is that of CAD, whereas the output format is that of CFD, and, thus, it may vary to fit CFD specifications. Logistically, in the framework of the considered technology, two types of operators are applied to the geometry: the operator of shape modification and the operator of change in the geometry format. To satisfy the earlier described requirements of the design technology, it is necessary to ensure the accuracy, robustness, low time, and low cost expenses for all of the operators involved in the geometry handling.

For example, consider the operator of grid construction. Note that every change in the geometry necessitates a new computational grid. With the conventional approach, the grids are constructed manually by means of commercially available grid generators. For a complex configuration, the time needed for this operation is measured by days. This manual technology is prohibitive where the number of tested geometries is high. To make the operation feasible in terms of time, it is crucial to reduce the manual labor to a minimum and to perform a large share of grid construction in an automatic way.

Another example is the CFD analysis of tested shapes. Where the number of runs involved in the preliminary design cycle is measured by hundreds, the time needed for a single CFD analysis should not be higher than a few hours. This means that a CFD tool used in the design cycle should be computationally efficient while remaining accurate and robust.

With the preceding requirements in view, the technology was developed that allows accomplishment of the major objectives of the preliminary design cycle. The description of this technology is given step by step.

The first step is to get a CAD representation of the aircraft configuration that comes from the conceptual design cycle. In our case, this may be a Unigraphics or CATIA representation. The second technology step is to prepare input data for the automatic optimizer OPTIMAS.

In the framework of the second step, the first action is to extract the geometry of the representative wing sections and the wing planform in the format of Cartesian coordinates (x, y, z).

The next action is to determine the Bezier spline coefficients for the aforementioned wing airfoils. This is performed automatically by means of a simple numerical procedure developed at IAI. This procedure is based on solving a problem of minimization by means of an efficient and robust genetic search.

The third action is to construct a computational wing grid that corresponds to the considered planform (needed for the CFD analysis in the framework of OPTIMAS). This grid is also constructed automatically starting from the universal wing grid that was developed manually (using GRIDGEN software).

This generic grid is of $C-O$ structure, and it comprises $161 \times 33 \times 37$ points in the chordwise, normal-to-surface, and spanwise directions, respectively. Existing experience shows that, due to a high-accuracy scheme employed in NES for full Navier–Stokes simulation, such grids ensure the sufficient accuracy for optimization purposes (see Ref. 23).

The final (fourth) action is to determine the flight conditions at the main and secondary design points, together with geometrical and aerodynamic constraints. Thus, we obtain all of the information required to form a single input file needed to start up the optimization technology step.

The engineering practice shows that an aerodynamic engineer is able to perform the above four actions and to prepare an input file in 1–2 working days. (third)

The next technology step consists of running the optimizer OPTIMAS. From the user viewpoint, the optimizer is a sort of the black box and the user (an aerodynamic engineer) is not supposed to tune the code by changing parameters of the optimizer.

Because as already mentioned the optimization code represents a highly parallelized software package, a multiprocessor cluster is required for its implementation. Specifically at IAI, a cluster of MIMD multiprocessors consisting of 228 nodes was employed. Each node has two processors, 2-GB RAM memory, 512-kB level 2 cache memory, and a full duplex 100-Mbps Ethernet interface. In total, this cluster contained 456 processors with 456-GB RAM and 114 MB level 2 cache memory.

One single-point optimization requires an overnight run on the aforementioned cluster. For example, a three-point optimization, which includes one main design point and two secondary design points, may take as much as 1.5–2 days.

As soon as the optimization process completes, it is necessary to attain aerodynamic data for the optimum shape (drag polars, Mach drag divergence curves, etc.). To obtain these data, massive CFD evaluations are required, and the overall time needed for this is measured by several days.

Thus, approximately one week after a given design task has been determined, the project management has at hand the optimal wing geometry together with all of the needed related aerodynamic data.

The aerodynamic analysis of the data obtained may result in a partial modification of the design requirements. Specifically, secondary design points or their weight coefficients may be changed, the specific values of the existing constraints may be modified, additional constraints may be placed on the wing configuration, etc. In this case, a new design task is determined, the existing OPTIMAS input file is slightly modified, and the internal loop of optimization is repeated. In practice, 2–3 such optimization processes are needed to obtain a wing that fully satisfies the project goals and, thus, to complete the third technology step.

The next technology step consists of the incorporation of the designed wing geometry into the full aircraft configuration. In this step, the first action is to transform the output OPTIMAS format of the optimized wing into an input CAD format. This is automatically done by a special procedure that takes only a few seconds. The second action consists of a CAD procedure that replaces the existing wing with the modified one. This is performed manually and may take up to several hours.

Finally, the full aircraft configuration is CFD tested to verify the overall aerodynamic effect. The most time consuming parts of this action are the construction of a new computational mesh for the complete configuration, which may take a couple of days, and the attainment of an extensive aerodynamic database by means of CFD computations. This may take up to 1 week on a cluster of 456 processors fully dedicated to this task.

It is clear that the incorporation of the wing into the complete aircraft may be performed in different ways even in the framework of the existing conceptual design solution. Usually, several alternatives are elaborated on with different aerodynamic trade-offs. Thus, the successfull incorporation of the wing into the complete aircraft may necessitate a number of CAD steps.

In summary, the cost of the described wing design technology in terms of time and human resources may vary from four to six weeks with a design team of 2–3 aerodynamicists.

IV. Analysis of Results

In this section we present a succession of various wing designs. The first group of examples verifies the method by applying it to two markedly different test cases.

The first test case is that of the European AEROSHAPE project (a multipoint two-dimensional optimization of an RAE2822 airfoil). This test case combines different flight conditions that impose contradictory requirements on the optimal shape.

The second test case deals with the optimization of a classical ONERA M6 wing in transonic conditions. The original ONERA M6 wing was not designed for real flight, and so, in principle, it can be rather easily improved in terms of drag. Nevertheless, this test case is a challenging one due to a low aspect ratio of the wing that results in an essentially three-dimensional flow behavior. This makes almost prohibitive any approach based on the optimization of two-dimensional airfoils followed by combining them in the wing by the methods popular in applied aerodynamics.

The second group of designs deals with the optimization of isolated wings. We have chosen two well-known wings: the wing of DLR F4 configuration and the wing of a Dornier 728 aircraft.

A. Verification Studies

The first example of the verification was the following multipoint optimization of an RAE2822 airfoil. The main design point was $M = 0.734$, $C_L = 0.8$, and $Re = 6.5 \times 10^6$ whereas the secondary design points were $M = 0.754$, $C_L = 0.74$, and $Re = 6.2 \times 10^6$ and $M = 0.680$, $C_L = 0.56$, and $Re = 5.7 \times 10^6$. The target was to minimize a weighted combination of total drag values at the design points with the following weight coefficients: $w_1 = 0.5$, $w_2 = 0.25$, and $w_3 = 0.25$, respectively. The constraints were imposed on the airfoil thickness and leading-edge radius, which cannot decrease. The case served for verification purposes in a number of studies, most recently performed within the European AEROSHAPE project and presented in Ref. 24.

The comparison of drag reduction achieved by the current optimization tool OPTIMAS with the corresponding AEROSHAPE results is summarized in Table 1.

Note that OPTIMAS achieves an essentially higher drag reduction, especially at the high transonic flight conditions. A detailed analysis shows that this is attributed to a successful shock destruction that allowed for the elimination of most of the wave drag.

The second example deals with the application of OPTIMAS to the design of ONERA M6 wing. The value of the relative thickness was not allowed to be lower than that of the original ONERA M6 wing, whereas the value of the relative leading-edge radius was allowed to be lower than the original one. The set of computational grids contained three multigrid levels. Each level included eight blocks. The total number of points in the fine level was close to 200,000.

This wing was employed as a three-dimensional optimization test case by a number of authors. In this work, a comparison with results presented by Weinerfelt[25] and Nielson and Anderson[26] was carried out. In Ref. 25, the CFD driver was an Euler solver, whereas the optimizer was gradient based. In Ref. 26, the CFD simulation was that of the full Navier–Stokes gasdynamic model, and the optimizer employed a discrete adjoint method. To allow for a consistent comparison, we performed the optimization at the design point $C_L = 0.3$ and $M = 0.84$ by both Euler and full Navier–Stokes CFD drivers.

Table 1 Drag reduction (counts) for multipoint transonic test case, one aerodynamic count = 0.0001

Design point	OPTIMAS	Ref. 24
$M = 0.734$, $C_L = 0.80$	−59.0	−40.0
$M = 0.754$, $C_L = 0.74$	−103.0	−34.0
$M = 0.680$, $C_L = 0.56$	+2.0	+3.0

The results of comparison are as follows. In Ref. 25 (Euler CFD driver), an initial pressure drag of 153 aerodynamic counts was reduced by 34 counts, to a level of 119 counts. In the present Euler-driven optimization, the reduction of pressure drag was equal to 53 counts (from the original 148.1 counts to 95.1 counts).

In Ref. 26 (a full Navier–Stokes driver), an initial total drag of 200 counts was reduced by 16 counts to a level of 184 counts. The present method (applied in the Navier–Stokes mode) yielded a reduction of 51 counts in the value of total drag (from 195.4 to 144.4 counts).

We may conclude that whereas the drag estimated by the foregoing codes for the initial ONERA M6 configuration are close one to another, the drag reduction by the present method is significantly higher.

B. Optimization of DLR-F4 Wing

In the following text, we present the results of one- and multipoint drag minimization of a DLR-F4 wing.[27] The main design point was $C_L = 0.5$ and $M = 0.75$. The secondary design points were chosen at $M = 0.8$ ($C_L = 0.5$) and at $M = 0.2$ ($C_L = 1.42$). The geometrical constraints (per section) were placed on relative thickness, relative leading-edge radius, and trailing-edge angle, as well as relative local thickness at two fixed x/c locations (beams constraints). An additional (aerodynamic) constraint was imposed on the value of pitching moment. The values of all of the constraints were kept to the level of the original DLR-F4 wing.

The design conditions and constraints are summarized in Table 2. The corresponding optimal wing shapes are designated as CaseDLR_1 and CaseDLR_2. The number of wing sections subject to design was equal to three (root, crank, and tip).

The original wing possesses good lift vs drag characteristics at the main design point $M = 0.75$ and $C_L = 0.5$. The total drag value at these conditions is $C_D = 167$ aerodynamic counts, whereas the theoretical induced drag amounts to $C_D = 110$ counts, and the minimum drag value C_{D_0} is 50 counts. The analysis of the corresponding pressure distribution shows that at the minimum C_D point almost no wave drag is present. This means that the minimum possible drag value at $C_L = 0.5$ is roughly estimated by 160 counts.

The one-point design enables exact achievement of this goal ($C_D = 160$ counts). The pressure distributions on the upper wing surface are shown in Figs. 1 and 2 for the original and optimized wing, respectively. The corresponding chordwise pressure distributions at a crank station are compared in Figs. 3 and 4. The improvement in pressure distribution is evident even if it yielded a relatively modest drag reduction.

Table 2 DLR-F4 wing, optimization conditions and constraints

C_L^*	M	w_i	C_M^*	$(t/c)_1$	$(t/c)_2$	$(t/c)_3$
			CaseDLR_1			
0.500	0.75	1.0	−0.16	0.148	0.123	0.123
			CaseDLR_2			
0.500	0.75	0.75	−0.16	0.148	0.123	0.123
0.500	0.80	0.23	−0.17	0.148	0.123	0.123
1.420	0.20	0.02	−0.32	0.148	0.123	0.123

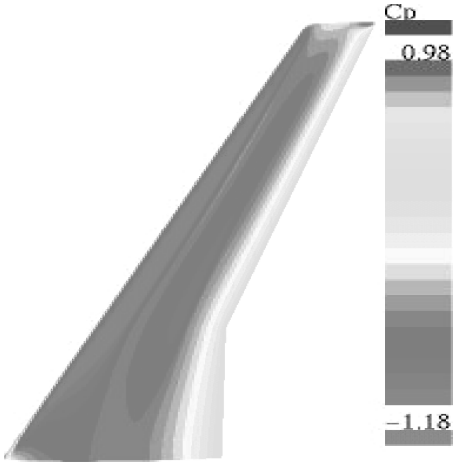

Fig. 1 Original DLR-F4 wing; pressure distribution on upper surface of wing at $M = 0.75$ and $C_L = 0.50$.

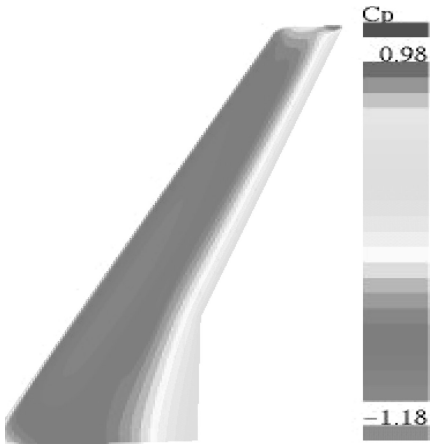

Fig. 2 Optimized DLR-F4 wing (CaseDLR_1); pressure distribution on upper surface of wing at $M = 0.75$ and $C_L = 0.50$.

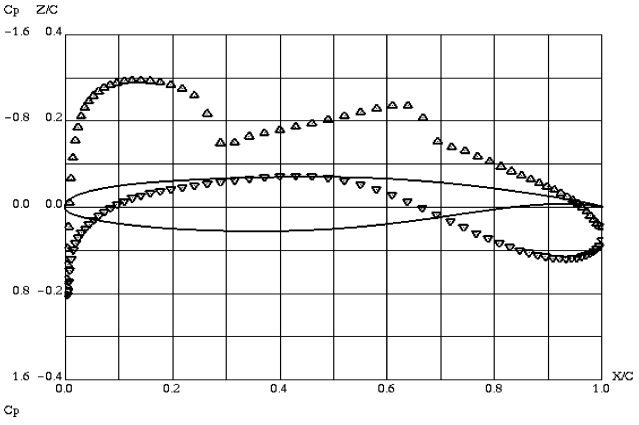

Fig. 3 Original DLR-F4 wing, $M = 0.75$ and $C_L = 0.5$; chordwise pressure distribution at wing crank station: ——, body geometry; △, C_p upper surface; and ▽, C_p lower surface.

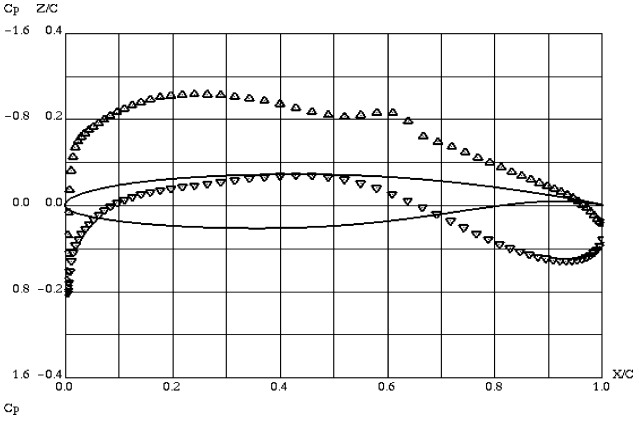

Fig. 4 Optimized DLR-F4 wing (CaseDLR_1), $M = 0.75$ and $C_L = 0.5$; chordwise pressure distribution at wing crank station: ——, body geometry; △, C_p upper surface; and ▽, C_p lower surface.

Thus, the aerodynamic analysis of the wing optimized at the main design point shows an improvement to the original wing. However, at a higher Mach zone, the performance is degraded in terms of drag: For example, at the same $C_L = 0.5$ and $M = 0.80$, the drag was augmented by 35 counts, from 205 to 240 counts. This means that (at least in the current case) the single-point design does not ensure good off-design Mach performance. To improve the design,

it appeared necessary to perform a multipoint optimization with the two secondary design points indicated earlier. The first of the additional design points is supposed to shift the Mach drag divergence point to a higher Mach zone, whereas the second point is required not to deteriorate the maximum lift value at the takeoff conditions.

The results of the corresponding three-point optimization (CaseDLR_2) are presented in Figs. 5–15. The multipoint optimization slightly improved the drag at the main design point, whereas at $M = 0.8$ and $C_L = 0.5$ the drag reduction was equal to 22 counts (from the original 205 counts down to 183 counts). This is shown in

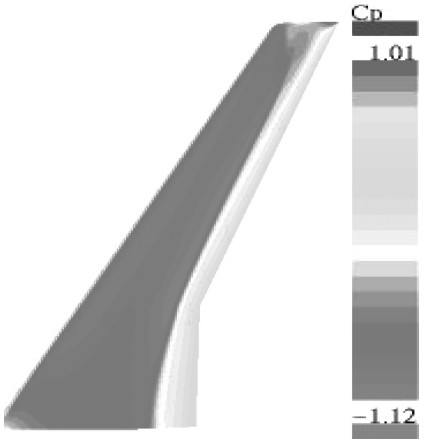

Fig. 5 Original DLR-F4 wing; pressure distribution on upper surface of wing at $M = 0.80$ and $C_L = 0.50$.

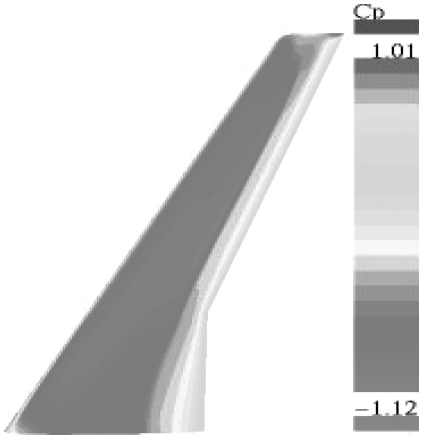

Fig. 6 Optimized DLR-F4 wing (CaseDLR_2); pressure distribution on upper surface of wing at $M = 0.80$ and $C_L = 0.50$.

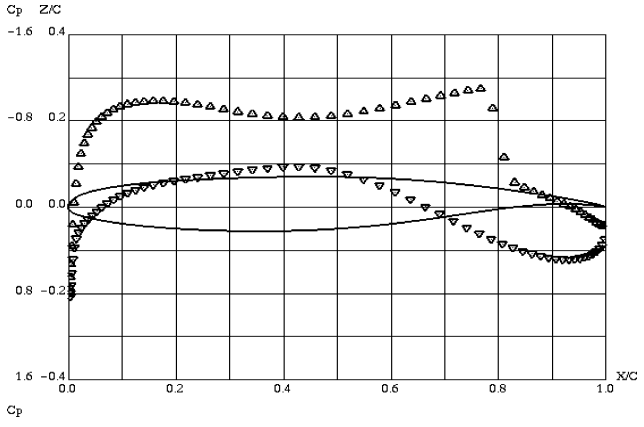

Fig. 7 Original DLR-F4 wing, $M = 0.8$ and $C_L = 0.5$; chordwise pressure distribution at wing crank station: ——, body geometry; △, C_p upper surface; and ▽, C_p lower surface.

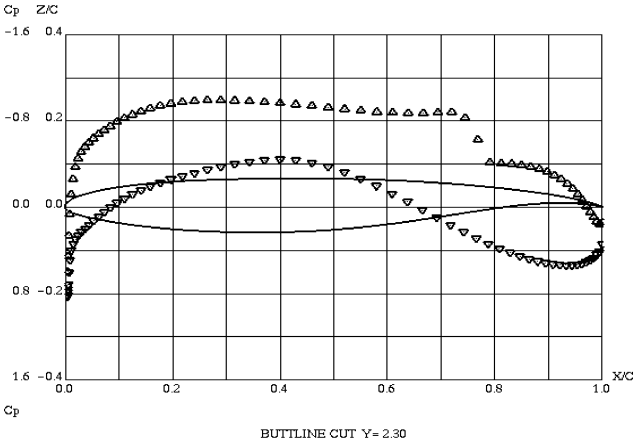

Fig. 8 Optimized DLR-F4 wing (CaseDLR_2), $M = 0.8$ and $C_L = 0.5$; chordwise pressure distribution at wing crank station: ——, body geometry; △, C_p upper surface; and ▽, C_p lower surface.

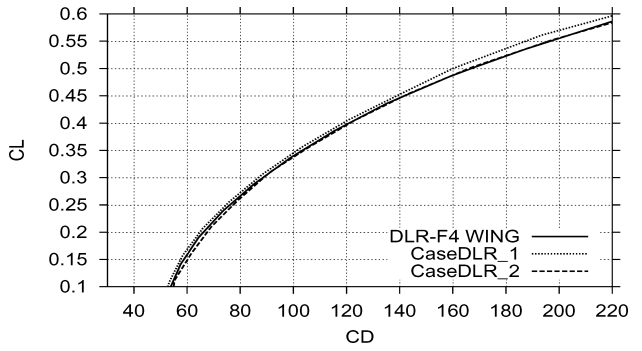

Fig. 9 DLR-F4 wing, drag polars at $M = 0.75$; one- and three-point optimizations vs original wing.

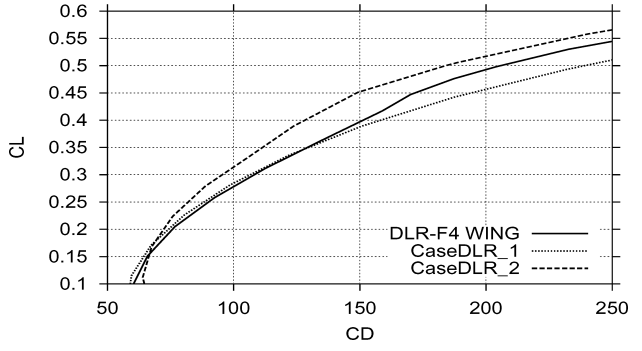

Fig. 10 DLR-F4 wing, drag polars at $M = 0.80$; one- and three-point optimizations vs original wing.

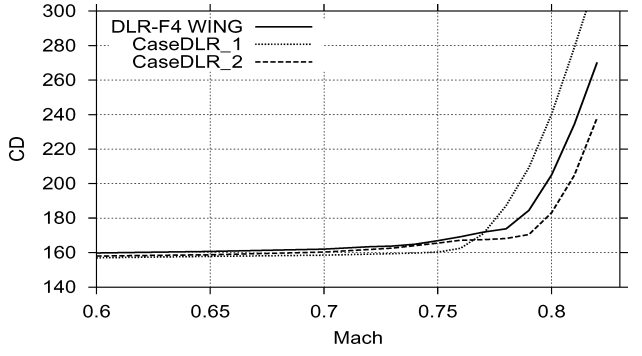

Fig. 11 DLR-F4 wing, Mach drag divergence curve at $C_L = 0.50$; one- and three-point optimizations vs original wing.

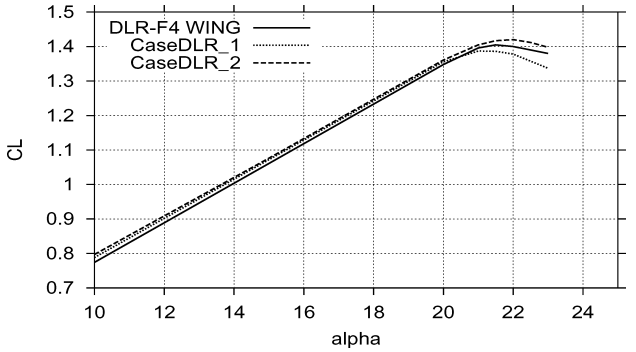

Fig. 12 DLR-F4 wing, C_L vs angle of attack α at $M = 0.20$.

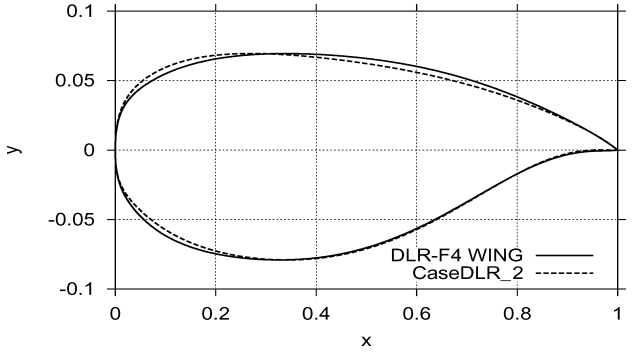

Fig. 13 Optimized DLR-F4 wing (CaseDLR_2), root shape.

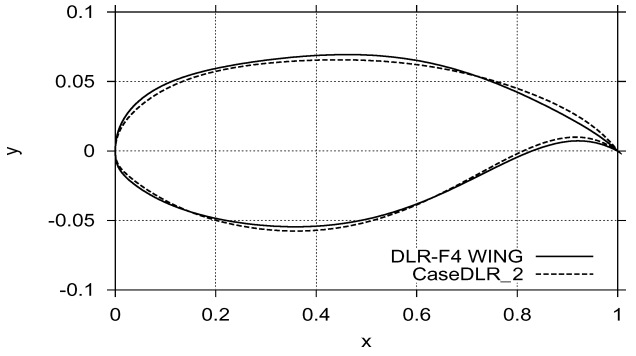

Fig. 14 Optimized DLR-F4 wing (CaseDLR_2), crank shape.

Figs. 5–8, where the pressure distribution on the upper surface of the wing and the chordwise pressure distribution at a crank station of the original wing are compared to those of the optimal one at $M = 0.80$. Note that the optimization resulted in the destruction of the original lambda shock and essentially decreased the shock strenth.

Lift/drag curves at $M = 0.75$ and 0.80 are shown in Figs. 9 and 10. At $M = 0.75$, the one-point optimization improved the lift/drag performance in the whole range of lift coefficients between $C_L = 0.1$ and 0.6. As for the three-point optimization, its polar at $M = 0.75$, which is close to the original one, possesses a slight but consistent improvement (about 1 count) in the vicinity of the design point. In the same time, the comparison at $M = 0.80$ demonstrates a clear superiority of the multipoint optimization shape over both the one-point optimization shape and the original wing.

The multipoint optimization slightly improved the drag value at the main design point while considerably extending the low drag zone at $C_L = 0.5$ from $M = 0.77$ to 0.80 and slightly improving $C_L^{\max}$ at takeoff conditions.

C. Optimization of Dornier-728 Wing

In this section we present the results of one- and multipoint drag minimization of Dornier-728 wing.[28] The main design point was $C_L = 0.5$ and $M = 0.78$. The secondary design points were chosen at $M = 0.8$ ($C_L = 0.5$) and at $M = 0.2$ ($C_L = 1.19$). Similar to DLR-F4 wing, the geometrical constraints were imposed on thickness, leading-edge radius, and trailing-edge angle alongside two beam constraints per section. An additional (aerodynamic) constraint was placed on the pitching moment.

Table 3 Dornier-728 wing, optimization conditions and constraints

C_L^*	M	w_i	C_M^*	$(t/c)_1$	$(t/c)_2$	$(t/c)_3$
			CaseD728_1			
0.500	0.78	1.0	−0.130	0.142	0.119	0.104
			CaseD728_2			
0.500	0.78	1.0	−0.072	0.142	0.119	0.104
			CaseD728_3			
0.500	0.78	0.75	−0.072	0.142	0.119	0.104
0.500	0.80	0.23	−0.082	0.142	0.119	0.104
1.190	0.20	0.02	−0.12	0.142	0.119	0.104

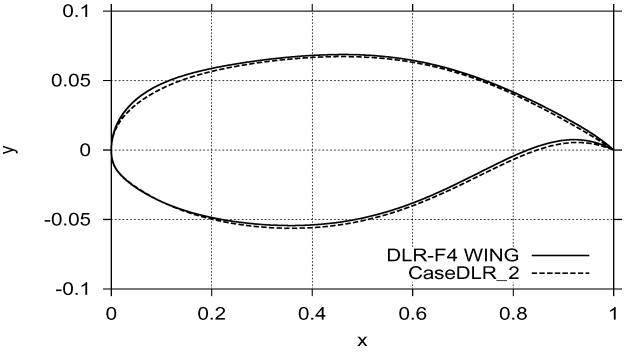

Fig. 15 Optimized DLR-F4 wing (CaseDLR_2), tip shape.

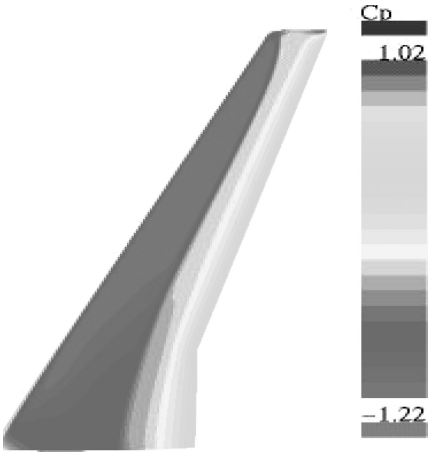

Fig. 16 Original Dornier-728 wing; pressure distribution on upper surface of wing at $M = 0.78$ and $C_L = 0.50$.

Design conditions and constraints are summarized in Table 3. A total of three optimizations were performed: two single-point optimizations and a three-point optimization. The number of wing sections subject to design was equal to three (root, crank, and tip). The single-point optimizations differ in the value of C_M^*. The first of the optimizations allowed for a loose pitching moment, whereas the second optimization (and the multipoint one) kept the pitching moment to the level of the original wing. The corresponding optimization cases are designated from CaseD728_1 to CaseD728_3.

The main design point lies in a high transonic range, where the flow over the original wing developes a strong shock (Fig. 16). The one-point optimization (CaseD728_1) eliminated the shock (Fig. 17). The corresponding chordwise pressure distributions are given in Figs. 18 and 19, respectively.

At these design conditions, a reduction of 32.6 counts was achieved (out of initial 213.7 counts). The minimum possible drag

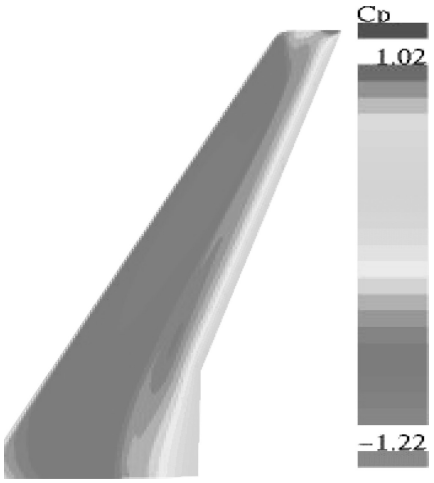

Fig. 17 Optimized Dornier-728 wing (CaseD728_1); pressure distribution on upper surface of wing at $M = 0.78$ and $C_L = 0.50$.

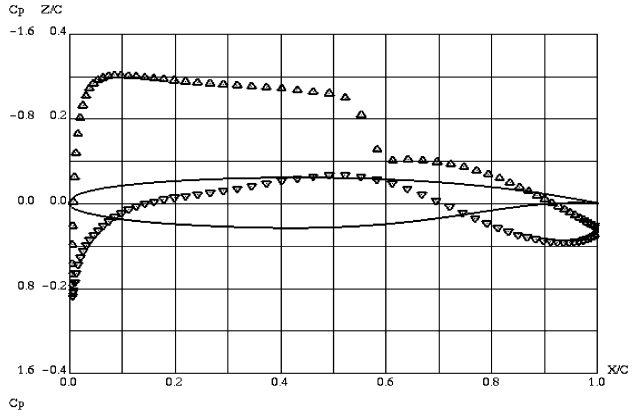

Fig. 18 Original Dornier-728 wing, $M = 0.78$ and $C_L = 0.5$; chordwise pressure distribution at wing station $y/b = 0.35$: ——, body geometry; △, C_p upper surface; and ▽, C_p lower surface.

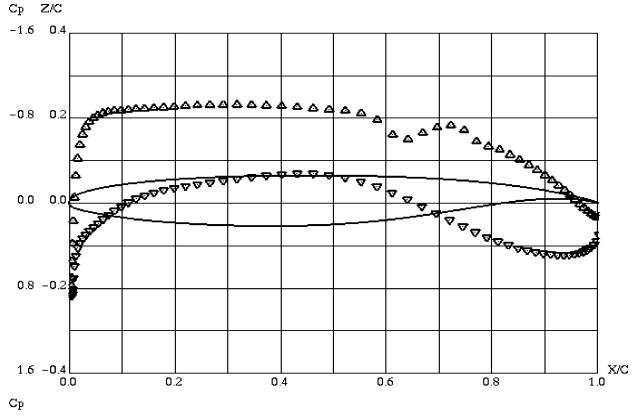

Fig. 19 Optimized Dornier-728 wing (CaseD728_1), $M = 0.78$ and $C_L = 0.5$; chordwise pressure distribution at wing station $y/b = 0.35$: ——, body geometry; △, C_p upper surface; and ▽, C_p lower surface.

value at this lift coefficient value is about 180 counts, which is practically identical to the drag of the optimized wing.

In this optimization case, the value of the pitching moment was allowed to travel rather far from that of the original wing. It was interesting to estimate the influence of this constraint on the results of optimization. A more restrictive pitching moment constraint ($C_M^* = -0.07$) placed on the optimization in CaseD728_2 resulted in a decrease in drag reduction: In this case, the total drag of the optimized wing is equal to 189.7 counts compared to 181.1 counts in CaseD728_1.

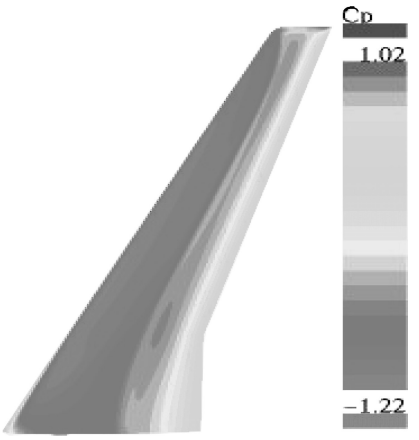

Fig. 20 Optimized Dornier-728 wing (CaseD728_3); pressure distribution on upper surface of wing at $M = 0.78$ and $C_L = 0.50$.

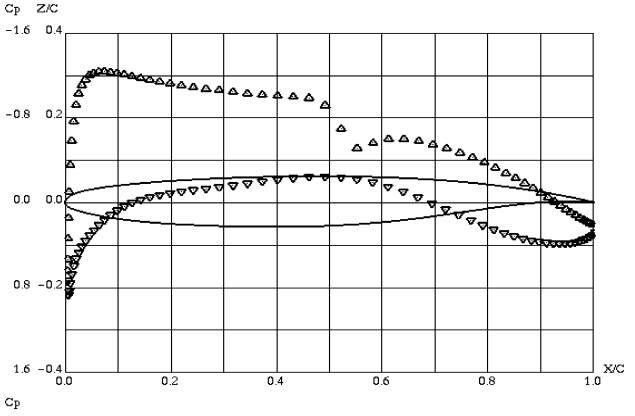

Fig. 21 Optimized Dornier-728 wing (CaseD728_3), $M = 0.78$ and $C_L = 0.5$; chordwise pressure distribution at wing station $y/b = 0.35$.

The off-design performance of the optimal shape of CaseD728_1 was satisfactory in terms of lift and drag characteristics, but it possesses too a high value of negative pitching moment. On the other hand, the optimization of CaseD728_2 has a suitable value of pitching moment due to the imposition of the corresponding constraint, but its takeoff performance deteriorated compared to that of the original wing. To ensure good design and off-design characteristics of the wing, we performed a multipoint optimization (CaseD728_3).

The results of the optimization are as follows: At the main design point ($C_L = 0.5$ and $M = 0.78$), the total drag of the optimized wing was equal to 192.8 counts, a value close to that of CaseD728_2. The corresponding pressure distribution on the upper surface of the wing is shown in Fig. 20, whereas the chordwise pressure distribution at a section close to the wing crank is shown in Fig. 21.

At the high-Mach secondary design point the drag amounts to 212.6 counts (compared to 244.1 counts of the initial wing and 216.7 counts of the CaseD728_2 shape). As seen from pressure distributions of Figs. 22–25, the original shock strength was diminished by the multipoint optimization.

The overall behavior of the optimized wings vs the original one is presented in Figs. 26–29. The lift/drag polar curves at $M = 0.78$ (Fig. 26) and at $M = 0.80$ (Fig. 27) show that the optimization allowed the improvement of aerodynamic performance at high lift coefficients ($C_L > 0.4$) without degrading the performance at lower C_L.

As for the Mach drag rise curves at cruise $C_L = 0.5$ (Fig. 28), the multipoint optimization resulted in a shift of the Mach drag divergence point to a higher Mach zone (from the original $M = 0.76$ to 0.80).

It was expected that the inclusion of the takeoff design point into the multipoint optimization should at least preserve the wing

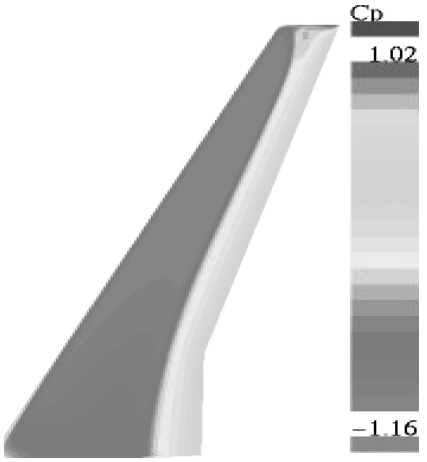

Fig. 22 Original Dornier-728 wing; pressure distribution on upper surface of wing at $M = 0.80$ and $C_L = 0.50$.

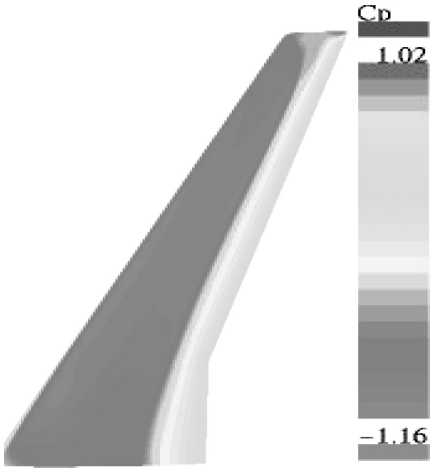

Fig. 23 Optimized Dornier-728 wing (CaseD728_3); pressure distribution on upper surface of wing at $M = 0.80$ and $C_L = 0.50$.

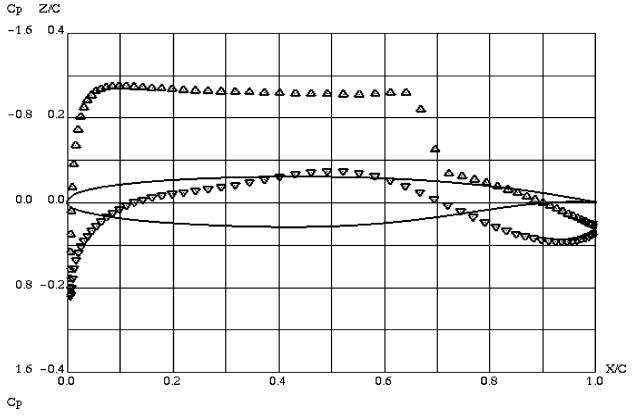

Fig. 24 Original Dornier-728 wing, $M = 0.80$ and $C_L = 0.5$; chordwise pressure distribution at wing station $y/b = 0.35$: ——, body geometry; △, C_p upper surface; and ▽, C_p lower surface.

high-lift characteristics at low Mach numbers. Indeed, the analysis of results confirmed this assumption (Fig. 29). In fact, the lift curve of the optimized wing is slightly better than the original one.

Finally, comparison between the optimized wing shapes (CaseD728_1 vs CaseD728_3) is shown in Figs. 30–32. The sectional airfoils corresponding to CaseD728_1 are predictably more cusped due to a greater allowed loading of the trailing-edge region of the wing (prompted by a weaker constraint on the pitching moment).

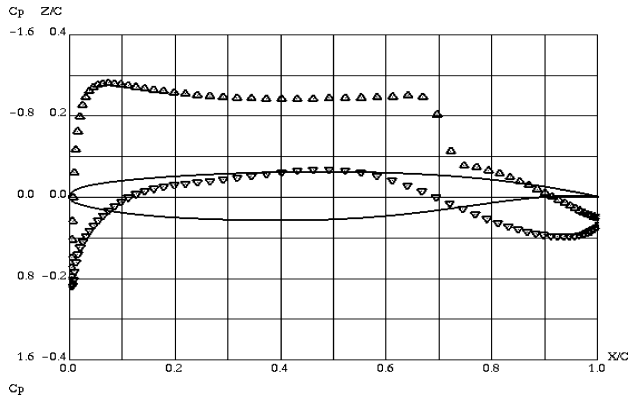

Fig. 25 Optimized Dornier-728 wing (CaseD728_3), $M = 0.80$ and $C_L = 0.5$; chordwise pressure distribution at wing station $y/b = 0.35$: ——, body geometry; △, C_p upper surface; and ▽, C_p lower surface.

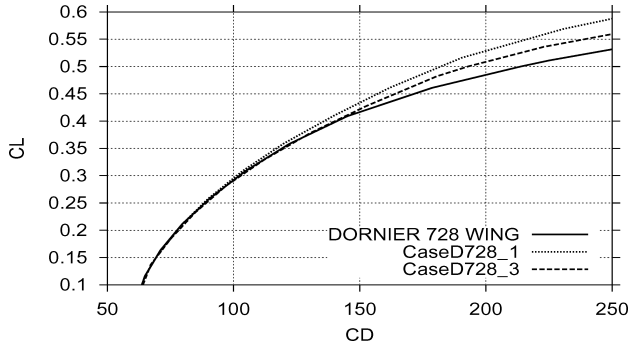

Fig. 26 Dornier-728 wing, drag polars at $M = 0.78$; one- and three-point optimizations vs original wing.

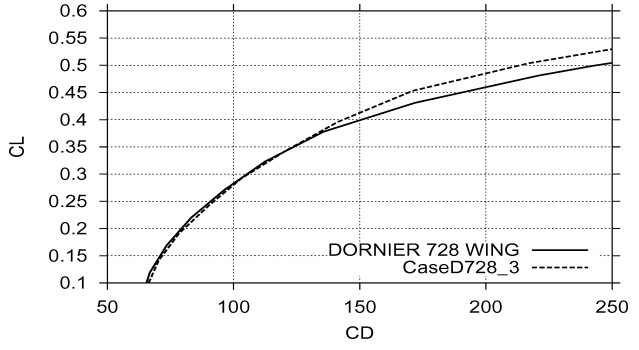

Fig. 27 Dornier-728 wing, drag polars at $M = 0.80$; three-point optimizations vs original wing.

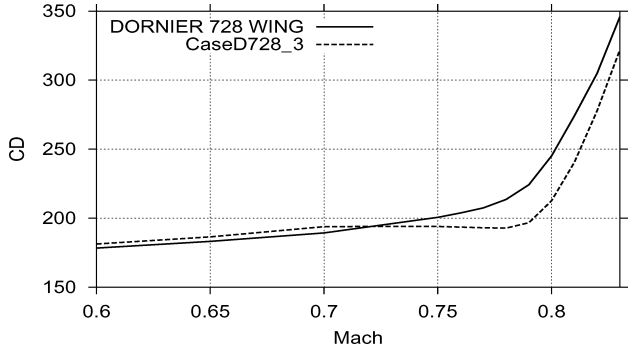

Fig. 28 Dornier-728 wing, Mach drag divergence curve at $C_L = 0.50$.

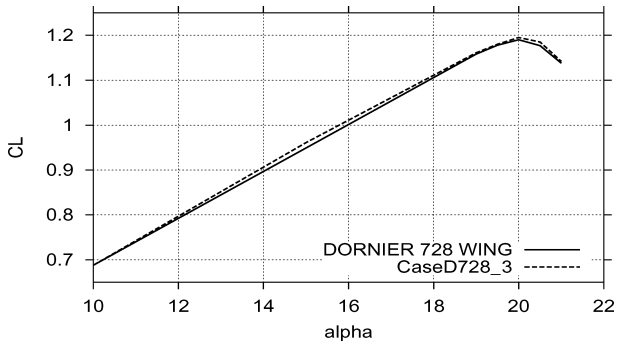

Fig. 29 Dornier-728 wing, C_L vs angle of attack at $M = 0.20$.

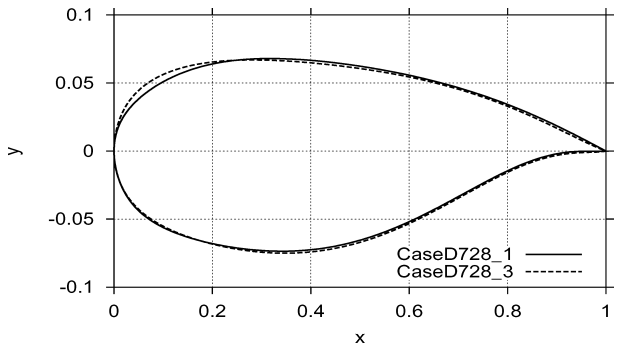

Fig. 30 Optimized Dornier-728 wing, CaseD728_1 vs CaseD728_3, root shape.

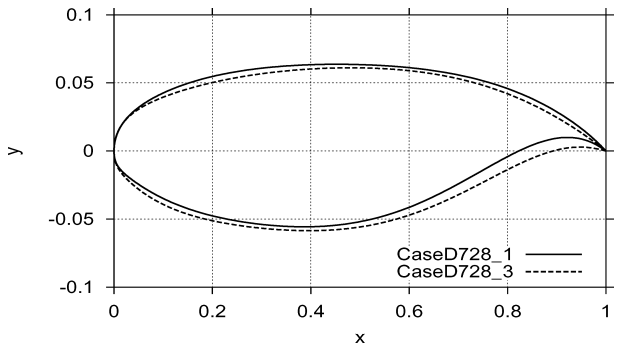

Fig. 31 Optimized Dornier-728 wing, CaseD728_1 vs CaseD728_3, crank shape.

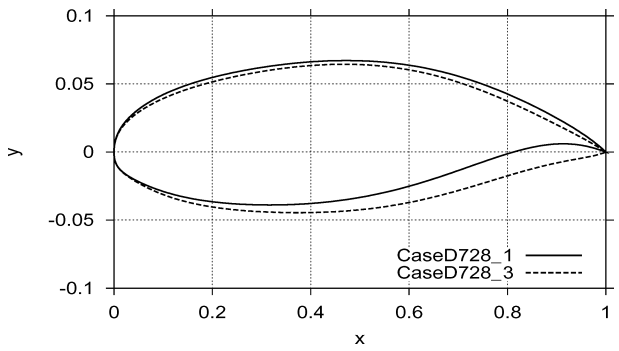

Fig. 32 Optimized Dornier-728 wing, CaseD728_1 vs CaseD728_3, tip shape.

V. Conclusions

A new method for optimization of aerodynamic shapes is applied to the multipoint design of three-dimesional transport-type wings. The method is based on CFD-driven constrained optimization to minimum drag through the use of the optimization tool OPTIMAS recently developed by the authors. The algorithm includes an efficient treatment of nonlinear constraints in the framework of GAs and scanning of the optimization search space by a combination of full Navier–Stokes computations with the ROM method, along with an efficient multilevel parallelization strategy. The results show that the multipoint multiconstrained optimization allows for essential improvements in aerodynamic performance at design and off-design flight conditions.

References

[1]Lighthill, M. J., "A New Method of Two-Dimensional Aerodynamic Design," Aeronautical Research Council, Rend M 2112, 1945.

[2]Bauer, F., Garabedian, P., Korn, D., and Jameson, A., *Supercritical Wing Sections II*, Springer-Verlag, New York, 1975, p. 296.

[3]Hicks, R. M., and Henne, P. A., "Wing Design by Numerical Optimization," *Journal of Aircraft*, Vol. 15, No. 4, 1978, pp. 407–412.

[4]*Optimum Design Methods for Aerodynamics*, R-803, AGARD 1994.

[5]Jameson, A., *Optimum Aerodynamic Design Using Control Theory*, CFD Review, Wiley, New York, 1995, pp. 495–528.

[6]Hajela, P., "Nongradient Methods in Multidisciplinary Design Optimization: Status and Potential," *Journal of Aircraft*, Vol. 36, No. 1, 1999, pp. 255–265.

[7]Jameson, A., Martinelli, L., and Vassberg, J., "Using Computational Fluid Dynamics for Aerodynamics—A Critical Assessment," *Proceedings of ICAS* 2002, Paper ICAS 2002-1.10.1, Optimage Ltd., Edinburgh, Scotland, U.K., 2002.

[8]Nadarajah, S. K., and Jameson, A., "Studies of the Continuous and Discrete Adjoint Approaches to Viscous Automatic Aerodynamic Shape Optimization," AIAA Paper 2001-2530, June 2001.

[9]Mohammadi, B., and Pironneau, O., *Applied Shape Optimization for Fluids*, Oxford Univ. Press, Oxford, England, U.K., 2001, p. 268.

[10]Vicini, A., and Quagliarella, D., "Inverse and Direct Airfoil Design Using a Multiobjective Genetic Algorithm," *AIAA Journal*, Vol. 35, No. 9, 1997, pp. 1499–1505.

[11]Obayashi, S., Yamaguchi, Y., and Nakamura, T., "Multiobjective Genetic Algorithm for Multidisciplinary Design of Transonic Wing Planform," *Journal of Aircraft*, Vol. 34, No. 5, 1997, pp. 690–693.

[12]Johnson, F. T., Tinoco, E. N., and Yu, N. J., "Thirty Years of Development and Application of CFD at Boeing Commercial Airplanes, Seattle," AIAA Paper 2003-3439, 2003.

[13]Epstein, B., Rubin, T., and Seror, S., "Accurate Multiblock Navier–Stokes Solver for Complex Aerodynamic Configurations," *AIAA Journal*, Vol. 41, No. 4, 2003, pp. 582–594.

[14]Shu, C.-W., and Osher, S., "Efficient Implementation of Essentially Non-oscillatory Shock-Capturing Schemes," *Journal of Computational Physics*, Vol. 83, No. 1, 1989, pp. 32–78.

[15]Seror, S., Rubin, T., Peigin, S., and Epstein, B., "Implementation and Validation of the Spalart–Allmaras Turbulence Model for a Parallel CFD Code," *Journal of Aircraft*, Vol. 42, No. 1, 2005, pp. 179–188.

[16]Epstein, B., and Peigin, S., "Robust Hybrid Approach to Multiobjective Constarined Optimization in Aerodynamics," *AIAA Journal*, Vol. 42, No. 8, 2004, pp. 1572–1581.

[17]Epstein, B., and Peigin, S., "Constrained Aerodynamic Optimization of Three-Dimensional Wings Driven by Full Navier–Stokes Computations," *AIAA Journal*, Vol. 43, No. 9, 2005, pp. 1946–1957.

[18]Michalewicz, Z., *Genetic Algorithms + Data Structures = Evolution Programs*, Springer-Verlag, New York, 1996, p. 387.

[19]Sefrioui, M., Periaux, J., and Ganascia, J.-G., "Fast Convergence Thanks to Diversity," *Proceedings of the 5th Annual Conference on Evolutionary Programming*, MIT Press, Cambridge, MA, 1996, pp. 321–335.

[20]Peigin, S., and Epstein, B., "Robust Optimization of 2D Airfoils Driven by Full Navier–Stokes Computations," *Computers and Fluids*, Vol. 33, No. 9, 2004, pp. 1175–1200.

[21]Peigin, S., and Epstein, B., "Embedded Parallelization Approach for Optimization in Aerodynamic Design," *Journal of Supercomputing*, Vol. 29, No. 3, 2004, pp. 243–263.

[22]Peigin, S., Epstein, B., Rubin, T., and Seror, S., "Parallel Large Scale High Accuracy Navier–Stokes Computations on Distributed Memory Clusters," *Journal of Supercomputing*, Vol. 27, No. 1, 2004, pp. 49–68.

[23]Peigin, S., and Epstein, B., "Robust Handling of Non-Linear Constraints for GA Optimization of Aerodynamic Shapes," *International Journal for Numerical Methods in Fluids*, Vol. 45, No. 11, 2004, pp. 1339–1362.

[24]Quagliarella, D., "Airfoil Design Using Navier–Stokes Equations and an Asymmetric Multi-Objective Genetic Algorithm," *Proceedings of 5th EUROGEN Conference*, CIMNE, Barcelona, Sept. 2003, pp. 43–45.

[25]Weinerfelt, P., "Gradient Based Optimization of ONERA M6 Wing," *INGENET Workshop*, Jan. 2000.

[26]Nielson, E., and Anderson, W., "Aerodynamic Design Optimization on Unstructured Meshes Using the Navier–Stokes Equations," AIAA Paper 98-4809, Sept. 1998.

[27]*A Selection of Experimental Test Cases for the Validation of CFD Codes*, Vol. 2, AR-303, AGARD, 1994, pp. 1–57.

[28]URL: http://www.nasq.com/afdb [cited 17 Oct. 2004].